Behavioral/Systems/Cognitive

Neural Specificity Predicts Fluid Processing Ability in Older Adults

Joonkoo Park,[1] Joshua Carp,[1] Andrew Hebrank,[2] Denise C. Park,[2] and Thad A. Polk[1]

[1]Department of Psychology, University of Michigan, Ann Arbor, Michigan 48109, and [2]The Center for Vital Longevity, University of Texas at Dallas, Dallas, Texas 75235

We investigated whether individual differences in neural specificity—the distinctiveness of different neural representations—could explain individual differences in cognitive performance in older adults. Neural specificity was estimated based on how accurately multivariate pattern analysis identified neural activation patterns associated with specific experimental conditions. Neural specificity calculated from a same/different task on two categories of visual stimuli (faces and houses) significantly predicted performance on a range of fluid processing behavioral tasks (dot-comparison, digit-symbol, Trails-A, Trails-B, verbal-fluency) in older adults, whereas it did not correlate with a measure of crystallized knowledge (Shipley-vocabulary). In addition, the neural specificity measure accounted for 30% of the variance in a composite measure of fluid processing ability. These results are consistent with the hypothesis that loss of neural specificity, or dedifferentiation, contributes to reduced fluid processing ability in old age.

Introduction

Measures of fluid processing abilities, such as speed of processing and executive function, tend to decline with age compared with measures of crystallized knowledge (e.g., vocabulary, world knowledge) (Salthouse, 1996; Park et al., 2002). Nevertheless, there is substantial variability in the cognitive performance of healthy older adults on fluid processing tasks. Some (even otherwise healthy) older adults exhibit significant declines in cognitive function, while others show comparable performance to young adults (Christensen et al., 1999; Hultsch et al., 2002). What distinguishes older adults who continue to perform well from older adults who do not?

One possibility is neural specificity—the extent to which the neural representations for two or more stimuli can be distinguished. Evidence suggests that neural representations that are very distinct in young adults are less distinct (more dedifferentiated) in older adults (Grady et al., 1994; Park et al., 2004). Converging evidence has found such age-related differences in neural specificity across a variety of tasks including visual object processing (Chee et al., 2006; Goh et al., 2010), working memory for pictures (Payer et al., 2006), and working memory for letters (Zarahn et al., 2007). Li et al. (2001) postulated that age-related decline in the distinctiveness of neural representations mediated behavioral deficits in fluid intelligence. Based on this framework, we hypothesized that individual differences in neural specificity in older adults would predict performance on a range of cognitive tasks that measured fluid processing ability.

Received Feb. 5, 2010; revised April 21, 2010; accepted May 25, 2010.

This work was supported by Grant 5R37AG006265-25 from the National Institute on Aging (to D.C.P.). We thank Patti Reuter-Lorenz for her helpful comments on an earlier version of this manuscript.

Correspondence should be addressed to Joonkoo Park, Department of Psychology, University of Michigan, 530 Church Street, Ann Arbor, MI 48109. E-mail: joonkoo@umich.edu.

DOI:10.1523/JNEUROSCI.0853-10.2010

 0270-6474/10/309253-07$15.00/0

Elderly participants first completed a battery of behavioral tasks designed to measure their fluid processing and crystallized knowledge. They then performed a simple visual task while neural activity was estimated using functional magnetic resonance imaging (fMRI). Neural specificity for the task was estimated based on how accurately a trained classifier could predict the stimulus category from the multivariate patterns of neural activation (Haynes and Rees, 2006; Norman et al., 2006). The relationship between neural specificity and various behavioral measures in older adults was examined using correlation and regression analyses. Because our hypotheses were about the impact of age on both cognitive behavior and neural specificity, we did not expect to see the same relationships in young adults, but we also tested a group of young for comparison purposes.

Materials and Methods

Subjects. Twenty-four healthy community-dwelling elderly from the Champaign-Urbana area participated in the study. Data from five of these participants were discarded because of excess motion, distortion due to improper head coil placement, vision problems, and/or failure to follow instructions, and the remaining 19 older adults (ages 61–69; 10 female; 15.89 mean years of education) were included in the analyses. Subjects had a minimum score of 26 on the Mini Mental State Examination (Folstein et al., 1975). Twenty-three younger adults were also recruited from the University of Illinois, matched by gender and years of education. Four younger subjects were discarded because of excessive motion during functional imaging, and data from the remaining 19 younger (ages 19–30; 10 female; 15.05 mean years of education) were included in the analyses. All participants were screened to ensure they were right-handed, native English speakers, psychologically and physically healthy, not taking medications with psychotropic or vascular effects, and free of any other MRI safety contraindications. All study procedures were reviewed and approved by the University of Illinois Institutional Review Board, and all participants provided detailed written consent before their involvement in this study.

Behavioral measures. Before scanning, participants completed a cognitive battery consisting of the WAIS Digit Symbol task ("digit-symbol") (Wechsler, 1981), Dot Comparison task ("dot-comparison") (Salthouse and Babcock, 1991), Trail-making tasks A and B ("Trails-A" and "Trails-B") (Reitan and Wolfson, 1993), and the Controlled Oral Association Task ("verbal-fluency") (Benton and Hamsher, 1976). The dependent measures were the number of symbols correctly copied in 90 s for digit-symbol, number of correct same/different comparisons in 45 s for three sections of dot-comparison, the time to complete the Trails for Trails-A (letters only) and Trails-B (alternating letters and numbers), and the number of unique F, A, and S words said in 60 s for each section of verbal-fluency. In addition, crystallized knowledge was measured using the Shipley Institute of Daily Living Scale ("Shipley-vocabulary") (Zachary, 1986). The dependent measure was the number of correct word-definition matches in a multiple choice test.

Experimental design and task. Each participant performed a simple visual task in the fMRI scanner. The visual task consisted of two six-min runs, each of which was organized into three 30 s "face" blocks and three 30 s "house" blocks in alternating order interleaved by 30 s "phase-scrambled" blocks. Each face block consisted of 15 trials (2 s each) in which participants viewed two grayscale images of faces presented side-by-side and were asked to make a same/different judgment. Likewise, each house block consisted of 15 trials in which participants viewed two grayscale images of houses presented side-by-side and were asked to make a same/different judgment. The task was the same in phase-scrambled blocks except that phase-scrambled images (preserving luminance and spatial frequencies but rendering the images visually meaningless) were used instead of faces or houses. For each trial, participants indicated "same" with their right index finger and "different" with their right middle finger. In the instructions, no emphasis was placed on either the speed or the accuracy of the judgment.

All visual stimuli were presented via E-prime (Psychology Software Tools) and displayed by a back-projection system. Responses were recorded using a Lumina response pad (Cedrus).

MRI data acquisition and preprocessing. Brain images were acquired with a 3T Siemens Allegra head-only system. A conventional echo-planar MR sequence was used for functional runs, with complete volumes acquired every 2 s [repetition time (TR) = 2000 ms, echo time (TE) = 25 ms, flip angle (FA) = 80°, field of view (FOV) = 220 mm]. Slices were 64 × 64 matrices acquired parallel to the AC-PC (anterior commissure-posterior commissure) line. Each volume consisted of 36 slices spanning 158 mm on the *z*-axis (encompassing all of the cerebrum and most of the cerebellum for most participants). A high-resolution (1 mm isotropic voxels) T1-weighted MPRAGE (magnetization-prepared rapid-acquisition gradient echo) was also acquired to facilitate warping individual volumes to atlas space.

Data were preprocessed using SPM5 (Wellcome Department of Cognitive Neurology, London, UK, www.fil.ion.ucl.ac.uk). Functional images underwent slice-timing correction and realignment to the mean volume. No normalization or spatial smoothing was applied.

We then estimated the neural response to each category relative to phase-scrambled control images using the general linear model (GLM). The model included separate regressors for each of the experimental blocks convolved with a canonical hemodynamic response function, as well as six nuisance covariates modeling head translation and rotation. This procedure yielded six estimates of face-evoked activation and six estimates of house-evoked activation.

Multivariate pattern analysis using support vector machine. We applied multivariate voxel selection and pattern analysis to identify brain regions that contribute to discriminating the experimental conditions in the whole brain and, at the same time, to assess the distinctiveness of the neural patterns. Machine learning algorithms, particularly linear-SVM (support vector machine), have been a popular tool in decoding neural activity (Kamitani and Tong, 2005; Li et al., 2007; Eger et al., 2008). They provide a measure of the distinctiveness of different patterns of neural activation, and they are also capable of selecting voxels that contribute to distinguishing the patterns (De Martino et al., 2008; Hanson and Halchenko, 2008). We used linear-SVM [using LIBSVM, C. C. Chang and C. J. Lin (2001) LIBSVM: a library for support vector machines. Software available at http://www.csie.ntu.edu.tw/~cjlin/libsvm] with recursive feature elimination (Guyon and Elisseeff, 2003; De Martino et al., 2008) to assess neural specificity associated with the task. All procedures were done on an individual subject basis.

Linear SVM finds a hyperplane that maximally separates trained neural patterns ($\boldsymbol{x}_i$) into two different labels (y_i, either 1 or −1). Mathematically, this is equivalent to minimizing $(1/2) \times \boldsymbol{w}^T\boldsymbol{w} + C\sum\xi_i$ subject to $y_i(\boldsymbol{w}\boldsymbol{x}_i + b) \geq 1 - \xi_i\,(i = 1, 2, \ldots, N; \xi \geq 0)$, where $\boldsymbol{w}$ is the weight vector, b is a bias value, ξ_i is a slack variable representing degree of misclassification, and C is a regularization parameter which was set to 1 for this analysis. Then, unknown neural patterns are classified according to the sign of the decision function $D(\boldsymbol{x}) = \boldsymbol{w}\boldsymbol{x} + b$, and the classification accuracy is computed as a measure of neural specificity. The magnitude of the weight w_j is related to the change in the objective function when voxel j is removed, and it effectively represents the contribution of voxel j to the classification performance (Guyon and Elisseeff, 2003).

Six whole-brain maps of face- and house-evoked activity were used in this classification procedure. A leave-one-out cross-validation approach with recursive feature elimination was used to assess the distinctiveness between face and house representations. In particular, one of the 12 patterns was left out while an SVM model was trained to fit the remaining 11 patterns. Next, a classifier was fit recursively while dropping uninformative voxels [i.e., voxels with weights (w_j) close to zero] until the number of final voxels reached 10%, 9.5%, 8% . . . 0.5% (decrementing by 0.5%) of the entire brain volume. Then, the left-out pattern was tested using only the selected voxels. This procedure was done iteratively with all 12 patterns. When the number of selected voxels was high (e.g., 10%; including many voxels that may not contribute well to the classification), many subjects' classification accuracies remained near chance level (0.5). When the number of selected voxels was low (e.g., 0.5%; including only a few critical voxels), many subjects' classification accuracies approached ceiling (1.0). We chose 6% of the entire brain volume so that every subject showed classification accuracy greater than chance while preserving maximum variability across subjects.

We verified the validity of the procedure by examining the null distribution of the classification accuracy for each subject. Specifically, we repeated the above procedure 200 times while permuting the category assignment for each pattern. There was no difference between the age groups in the mean classification accuracy of this null distribution ($t_{(36)} = 1.081$, $p = 0.144$, two-tailed) (supplemental Fig. S1, available at www.jneurosci.org as supplemental material).

Visualization of category-selective regions. The SVM classification with recursive feature elimination was performed on all 12 patterns without cross-validation to visually identify category-selective regions. A binary category-selective region of interest (ROI) (i.e., 1 if category-selective and 0 otherwise) was created for each individual in his or her native space based on the voxel selection criterion (6% of the entire brain volume). Each participant's binary map was then normalized using SPM5. Each participant's T1 anatomical image was coregistered with the functional images and then segmented into gray matter, white matter, and CSF. The gray matter was normalized into the default gray matter probability template in standard MNI (Montreal Neurological Institute) space, and the acquired normalization parameters were used to normalize the category-selective ROI maps for each individual.

To assess the statistical significance of each voxel, the normalized binary category-selective maps for each subject were spatially smoothed with a 3 voxel isotropic Gaussian kernel, and these maps were summed across all subjects. The probability distribution of the summed map under the null hypothesis was estimated using a permutation test (category- selective voxels were redistributed in random locations in each participant 2000 times). This distribution was then used to calculate a *z*-statistic at each voxel, based on the observed aggregated category-selective maps across all subjects (see Fig. 2).

Multivariate pattern analysis using correlation analysis. The SVM classification analysis is relatively coarse, with only 12 activation patterns to be predicted. This results in a total of only 13 possible values for the dependent measure (0/12, 1/12, 2/12 . . . 12/12), and only five unique

accuracy values were observed in our data with older adults (see Fig. 1), providing a coarse index of neural specificity. To compute a more fine-grained dependent measure as well as to evaluate the replicability of the findings, we obtained an additional measure of neural specificity using correlation analysis. This measure was first used by Haxby et al. (2001) and was recently used by Carp et al. (2010) to measure age differences in neural specificity. First, we used coefficient estimates of the GLM from two blocks for each category (second block of the first run and the second block of the second run for each category) and found regions in the whole brain that were significantly activated either by face compared with house or house compared with face ($p < 0.001$, uncorrected). These regions then served as a mask for each participant. We then extracted the patterns for faces in run1 and run2 and for houses in run1 and run2 (excluding the blocks that were used to create the mask) within this mask. Neural specificity was then defined as the difference between the Pearson correlation within-categories (i.e., the average of the correlation of face patterns between run1 and run2 and the correlation of house patterns between run1 and run2) and between-categories (i.e., the average of the correlation between the face pattern from run1 and the house pattern from run2 and the correlation between the face pattern from run2 and the house pattern from run1).

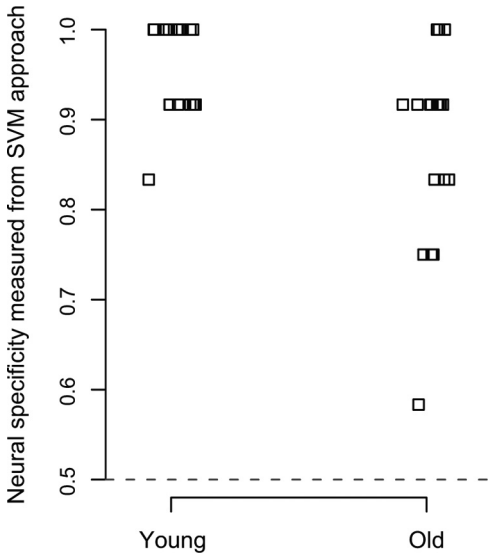

Figure 1. A dot plot of neural specificity of the visual activity measured as classification accuracy of a linear-SVM classifier. Neural specificity was significantly higher in the younger adults than in the older adults ($t_{(36)} = 3.268$, $p = 0.001$). Chance performance is 0.5, indicated with a gray dashed line.

Results

Cognitive performance measures

Replicating previous work (Park et al., 2002), older adults' performance on all the fluid processing tasks was worse than that of younger adults (digit-symbol, $t_{(36)} = 6.97$, $p < 0.001$; dot-comparison, $t_{(36)} = 5.52$, $p < 0.001$; verbal-fluency, $t_{(36)} = 1.95$, $p < 0.029$; Trails-A, $t_{(36)} = -0.584$, $p = 0.281$; Trails-B, $t_{(36)} = -1.78$, $p = 0.042$; but no age differences were observed on the crystallized knowledge test (Shipley-vocabulary, $t_{(36)} = -0.716$, $p = 0.761$) (Table 1).

Neural specificity measures

Neural specificity was defined as the accuracy of the trained classifier in predicting the category of the visual stimulus (face or house) based on the pattern of neural activation in the selected ROI.

Older adults showed decreased neural specificity ($t_{(36)} = 3.268$, $p = 0.001$) compared with the younger adults (Fig. 1). These results replicate previous studies of ventral visual dedifferentiation (Park et al., 2004; Payer et al., 2006) but extend them to measures of whole-brain function. The neural specificity measure was then used in subsequent regression analyses to examine the relationship between neural specificity and behavioral performance measures in the older adults.

Voxel selection and category-selective ROIs

Before examining the relationship between neural specificity and behavior, we visually inspected the anatomical locations of each subject's category-selective ROI determined by the multivariate voxel selection procedure. Category-selective ROIs were visualized by aggregating individual participants' ROIs in normalized space separately for each age group (see Materials and Methods). Figure 2 illustrates category-selective regions in the visual task of matching faces and houses ($p < 10^{-6}$, uncorrected). In both age groups, areas traditionally known as face-selective and house-selective such as the mid-fusiform and the parahippocampal gyri, as well as some extrastriate areas, were identified as category-selective regions.

Neural specificity and its behavioral correlates

Next, we tested our primary hypothesis that neural specificity predicts fluid processing in the older adults. Using correlation and regression analyses, we first examined the relationship between neural specificity and each of the individual behavioral measures. Controlling for age, neural specificity of visual activity significantly predicted performance on dot-comparison ($\beta = 36.803$, $t_{(16)} = 1.987$, $p = 0.032$), digit-symbol ($\beta = 53.296$, $t_{(16)} = 2.930$, $p = 0.005$), and verbal-fluency ($\beta = 28.926$, $t_{(16)} = 2.533$, $p = 0.011$), while Trails-A ($\beta = -59.184$, $t_{(16)} = -1.712$, $p = 0.053$) and Trails-B ($\beta = -104.073$, $t_{(16)} = -1.144$, $p = 0.135$) missed the 0.05 cutoff (Fig. 3*A*, one-tailed for all directional analyses unless otherwise noted).

With only 12 activation patterns the granularity of this measure of classification accuracy was low, and only five unique accuracy values were observed in our data with older adults (Fig. 1). To compute a more fine-grained dependent measure as well as to evaluate the replicability of the findings, we ran a second analysis using Pearson correlation measures (see Materials and Methods). This analysis revealed a trend toward greater specificity in younger adults compared with older adults, although this effect did not reach statistical significance ($t_{(36)} = 1.474$, $p = 0.075$) (supplemental Fig. S2, available at www.jneurosci.org as supplemental material). Nevertheless, the relationship between neural specificity measured using this correlation analysis and each of the

Table 1. Summary of demographic and behavioral measures

	Age***	Digit-symbol***	Dot-comparison***	Verbal fluency*	Trails A	Trails B*	Shipley vocabulary
Young ($N = 19$)	22.21 (0.55)	74.21 (2.45)	49.84 (2.14)	27.11 (1.79)	33.89 (2.60)	60.63 (5.22)	33.58 (0.71)
Old ($N = 19$)	64.79 (0.65)	52.47 (1.93)	34.47 (1.79)	22.95 (1.16)	36.32 (3.22)	77.79 (8.12)	34.42 (0.94)

The mean and SEM (in parentheses) are shown for each measure. Significant age differences are indicated by asterisks next to the name of each measure (*$p < 0.05$; ***$p < 0.001$; one-tailed for all directional analyses unless otherwise noted).

individual behavioral measures in older adults (Fig. 4*A*) showed striking similarity to the analysis that was based on the SVM. Controlling for age, neural specificity measured using this correlation analysis predicted performance on digit-symbol ($\beta = 21.449$, $t_{(16)} = 2.624$, $p = 0.009$), verbal-fluency ($\beta = 9.971$, $t_{(16)} = 1.880$, $p = 0.039$), Trails-A ($\beta = -26.748$, $t_{(16)} = -1.799$, $p = 0.045$) and Trails-B ($\beta = -68.484$, $t_{(16)} = -1.836$, $p = 0.043$), while the relationship with dot-comparison did not reach significance at the 0.05 level ($\beta = 11.020$, $t_{(16)} = 1.292$, $p = 0.108$) (Fig. 4*A*).

The five fluid processing measures (i.e., all the behavioral tasks except Shipley-vocabulary) were highly correlated with each other (Table 2), suggesting they depend on a shared construct. We used principal component analysis to reduce the dimension of these behavioral measures, and it yielded a single principal component. We termed this composite score fluid processing ability, and we assessed the relationship between neural specificity and this composite behavioral measure.

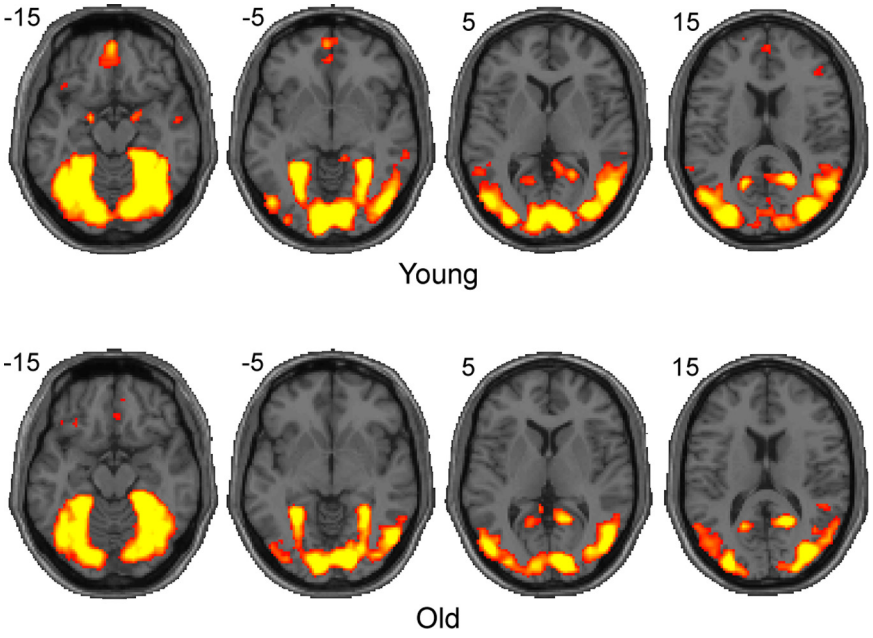

Figure 2. Visualization of category-selective ROIs determined by the multivariate voxel selection method. Category-selective ROIs from individual subjects were aggregated in the standard normalized MNI space to visualize the category-selective regions for the visual categories at the group level. Note that these are not activation maps. Colored areas indicate voxels that reliably contributed to distinguishing patterns of activity elicited by face versus house conditions (for the visual task) ($p < 10^{-6}$, uncorrected). The left hemisphere appears on the left. Coordinates for these axial slices are given in MNI space.

Figure 3*B* illustrates the relationship between this composite measure of fluid processing ability and the neural specificity measure in the older adults. Neural specificity significantly predicted fluid processing ability while controlling for age ($\beta = 10.806$, $t_{(16)} = 2.667$, $p = 0.008$). We obtained the same result when the neural specificity measure from the correlation-based analysis was used to predict the behavioral measure as shown in Figure 4*B* ($\beta = 4.368$, $t_{(16)} = 2.417$, $p = 0.014$) (see supplemental Figs. S3 and S4, available at www.jneurosci.org as supplemental material, for the results of the younger adults).

Because the blood oxygenation level-dependent (BOLD) signal is an indirect measure of neural activity, it is possible that our measure of neural specificity may be influenced by individual differences in vascular noise (D'Esposito et al., 2003). We therefore tested whether neural specificity could predict fluid processing after controlling for a measure of BOLD variability. We extracted the estimate of the error variance of the GLM model (residual mean squared from the SPM5 results) within the posterior cingulate cortex (a region we assumed was not strongly involved in distinguishing the face and place conditions) for each subject. A mask of the posterior cingulate cortex was created in standard MNI space using the PickAtlas toolbox (http://www.fmri.wfubmc.edu/cms/software), and this mask was inverse transformed to each participant's native space. Neural specificity still significantly predicted fluid processing ability when the median of the estimate of the error variance was included as a covariate in the model ($\beta = 11.233$, $t_{(15)} = 2.695$, $p = 0.008$, neural specificity measured from SVM approach; $\beta = 4.414$, $t_{(15)} = 2.374$, $p = 0.016$, neural specificity measured from correlation approach). These results suggest that the association between neural specificity and behavior is not attributable to individual differences in BOLD variability unrelated to task, which may be associated with vascular noise.

In contrast to the fluid measures, neural specificity showed no relationship with Shipley vocabulary score ($\beta = 1.1945$, $t_{(16)} = 0.110$, $p = 0.457$, neural specificity measured using SVM, Fig. 3*C*; $\beta = 1.240$, $t_{(15)} = 0.264$, $p = 0.398$, neural specificity measured using correlation analysis, Figure 4*C*), our measure of crystallized knowledge. In addition, using hierarchical linear regression, we found that the crystallized knowledge measure did not explain additional variance in neural specificity, above the variance explained by fluid processing ability in older adults (R^2 increment $= 0.042$, $F_{(1,16)} = 1.269$, $p = 0.278$, neural specificity measured from the SVM approach; R^2 increment $= 0.026$, $F_{(1,16)} = 0.633$, $p = 0.439$, neural specificity measured from the correlation approach).

Finally, we addressed the total variance explained in the two abilities by age alone and then added neural specificity in a hierarchical regression in older adults (Table 3). Age alone

Table 2. Correlation matrix for the five fluid processing tasks in the old

	Digit-symbol	Dot-comparison	Verbal fluency	Trails A	Trails B
Digit-symbol	1.000				
Dot-comparison	0.675**	1.000			
Verbal fluency	0.651**	0.734**	1.000		
Trails A	−0.532**	−0.511*	−0.642**	1.000	
Trails B	−0.480*	−0.338	−0.489*	0.690**	1.000
Shipley-vocabulary	0.213	0.265	0.486*	−0.396*	−0.348

*$p < 0.05$; **$p < 0.01$ (see supplemental Table S1, available at www.jneurosci.org as supplemental material, for the correlation matrix in the young).

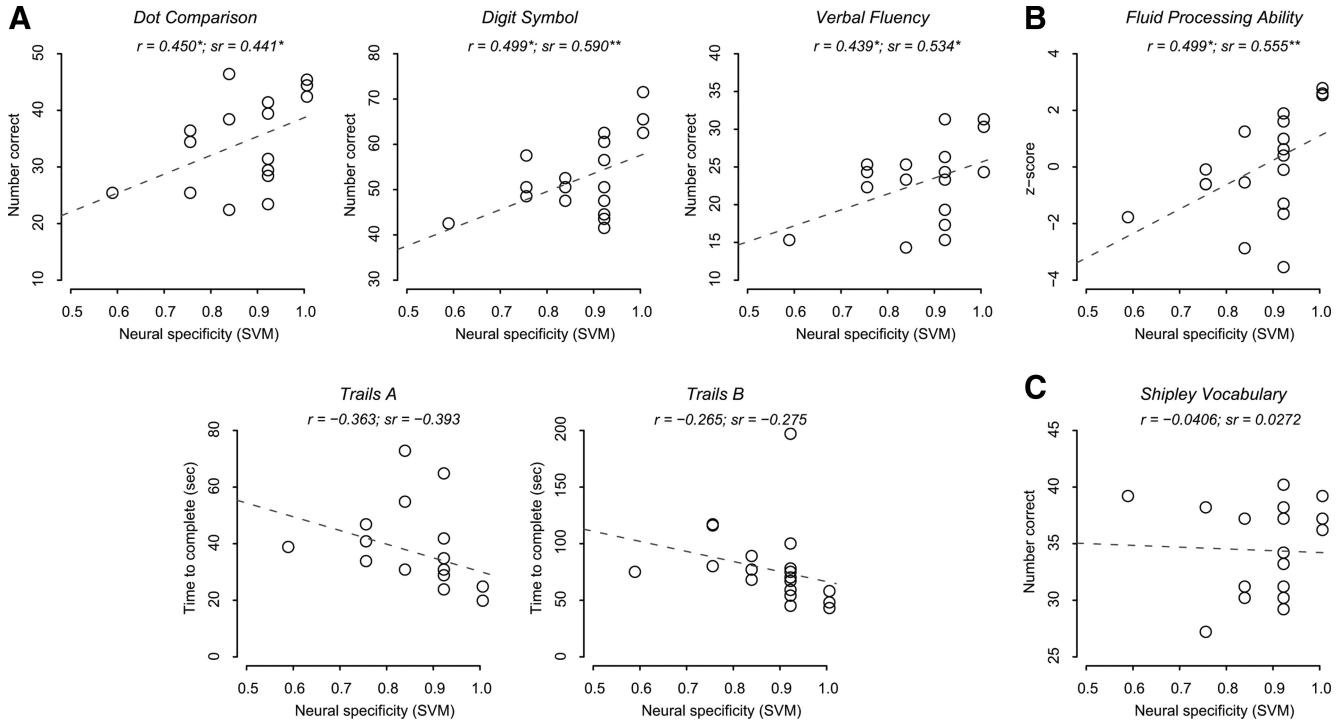

Figure 3. Scatter plots showing the relationship between the measure of neural specificity from the SVM approach and five fluid processing tasks (***A***), the composite measure of the fluid processing tasks (***B***), and a crystallized knowledge task (***C***) in older adults. Zero-order correlations (*r*) illustrate simple linear relationships between each behavioral measure and neural specificity; semipartial correlations (*sr*) illustrate the unique contribution of neural specificity in predicting a behavioral measure controlling for age (*$p < 0.05$; **$p < 0.01$; ***$p < 0.001$). In all plots, each data point represents a single older adult, and the gray dashed line indicates an ordinary least square linear fit.

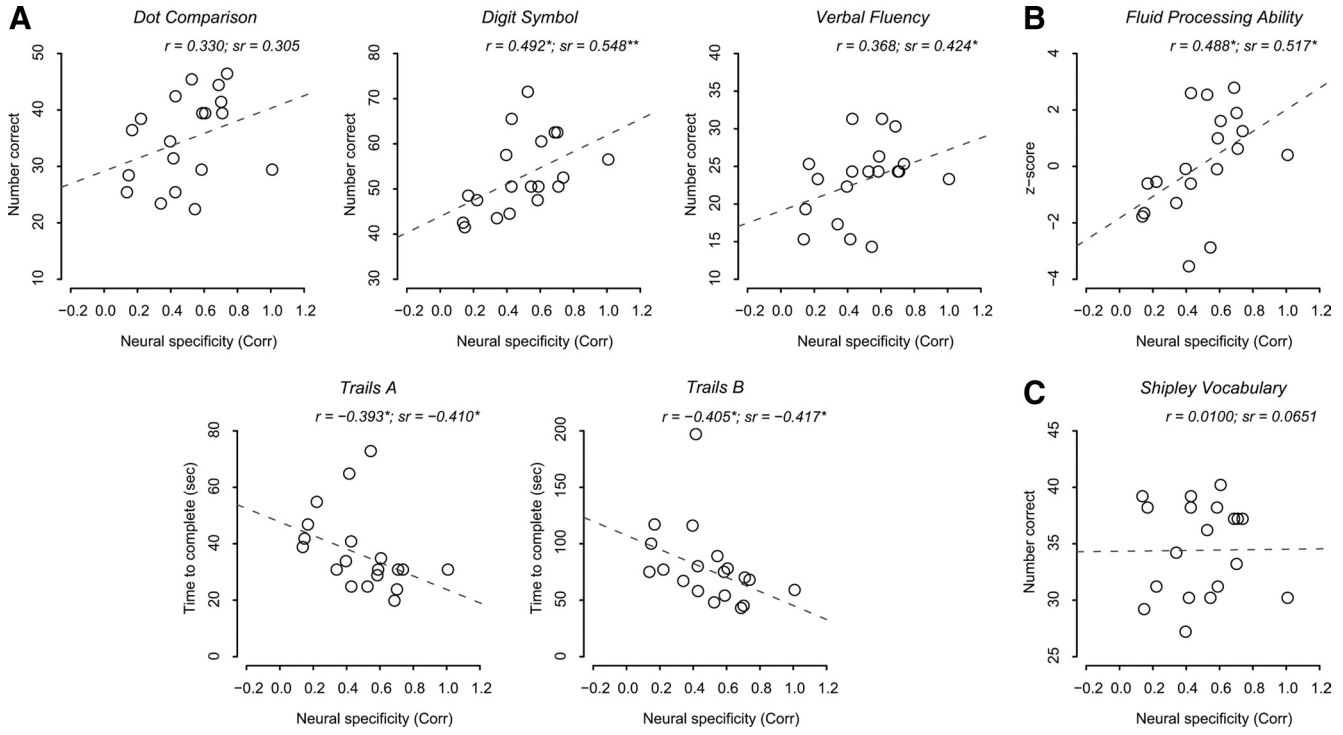

Figure 4. Scatter plots showing the relationship between the measure of neural specificity from the correlation approach and five fluid processing tasks (***A***), the composite measure of the fluid processing tasks (***B***), and a crystallized knowledge task (***C***) in older adults. Notational conventions are the same as in Figure 3.

explained <1% of the variance in fluid processing ability and ~2% of the variance in crystallized knowledge when entered in the first step. This is not surprising because the older subjects had a tight age range between 61 and 69. Importantly, in a second step after age, neural specificity from the SVM approach explained an additional 30.8% of the variance in fluid processing ability ($F_{(1,17)} = 7.114$, $p = 0.017$), but only produced a nonsignificant increment of <1% in the crystallized knowledge measure.

Table 3. Hierarchical regressions of fluid processing ability (composite measure) and crystallized knowledge in older adults

Model	Response	Step	Predictor(s)	R^2	df	F	p
A	Fluid processing ability	1	Age	0.0003	1,17	0.005	0.946
		2	+ Visual (SVM)	0.308	2,16	3.560	0.052
			R^2 increment	=0.308	1,17	7.114	0.017
B	Crystallized knowledge	1	Age	0.020	1,17	0.339	0.568
		2	+ Visual (SVM)	0.020	2,16	0.166	0.849
			R^2 increment	=0.0007	1,17	0.012	0.914
C	Fluid processing ability	1	Age	0.0003	1,17	0.005	0.946
		2	+ Visual (Corr)	0.268	2,16	2.924	0.083
			R^2 increment	=0.267	1,17	5.843	0.028
D	Crystallized knowledge	1	Age	0.020	1,17	0.339	0.568
		2	+ Visual (Corr)	0.024	2,16	0.195	0.825
			R^2 increment	=0.004	1,17	0.070	0.796

In model A, fluid processing ability was explained by age (first step) and the neural specificity measure from the SVM approach (second step). In model B, crystallized knowledge was explained by age (first step) and the neural specificity measure from the SVM approach (second step). R^2 increment represents the variance explained by the neural specificity measures beyond age. Models C and D are identical to A and B, respectively, except that the neural specificity measure from the correlation approach was used instead.

Discussion

In this study, we investigated whether individual differences in neural specificity could explain individual differences in cognitive performance in older adults. Although we were primarily interested in how levels of neural specificity predicted individual differences in older adults, we also collected data from younger adults to replicate previous findings of age-group differences in behavioral performance and neural specificity. As expected, older adults showed decreased performance in fluid processing tasks compared with younger adults while their performance in a crystallized knowledge task was comparable to that of younger adults (Table 1). Likewise, there was a group difference in the measure of neural specificity (Fig. 1; supplemental Fig. S2, available at www.jneurosci.org as supplemental material).

To test our primary hypothesis, we examined the relationship between neural specificity and various behavioral measures in older adults using correlation and regression analyses. We found that neural specificity in the older adults, measured using two different approaches, was significantly associated with measures of fluid processing ability, but not with crystallized knowledge. The failure to explain crystallized knowledge is of particular interest given that there was a moderate correlation between the Shipley-vocabulary score and fluid processing ability ($r = 0.421$, $t_{(17)} = 1.916$, $p = 0.073$, two-tailed), suggesting that the behavioral effect of neural specificity is unique to fluid processing ability. Furthermore, nearly 30% of the variance of fluid processing ability was explained by neural specificity in response to simple visual stimuli that have no obvious similarity to the psychometric measures collected outside of the scanner. These results suggest that neural specificity may be a fundamental neural measure associated with performance on complex cognitive tasks.

This interpretation is consistent with the hypothesis that age-related decline in the efficacy of neurotransmitter function and neuromodulation leads to less distinctive neural representations, which in turn underlie deficits in behavioral performance (Bäckman et al., 2000; Li et al., 2001; Li and Sikström, 2002). Our results demonstrate that variability in neural specificity within a group of older adults, possibly due to individual differences in neural noise during the processing of visual categories, is strongly related to individual differences in behavioral performance.

Of course, declines in neural specificity are just one type of age-related neural change. There are a number of others, including bilateral recruitment (Cabeza, 2002; Reuter-Lorenz, 2002) and suppression deficits in sensory cortex and default networks (Gazzaley et al., 2005; Park et al., 2010). These changes may be quite different from the sensorimotor specificity investigated in this study. Future work should study the relationship between these different types of neural change and their association with behavioral measures.

In conclusion, neural specificity predicts fluid processing ability in older adults. These findings demonstrate that declining neural specificity may play an important role in cognitive decline and that preserved neural specificity may even be an indicator of healthy cognitive aging.

References

Bäckman L, Ginovart N, Dixon RA, Wahlin TB, Wahlin A, Halldin C, Farde L (2000) Age-related cognitive deficits mediated by changes in the striatal dopamine system. Am J Psychiatry 157:635–637.

Benton A, Hamsher K (1976) Multilingual Aphasia Examination. Iowa City: University of Iowa.

Cabeza R (2002) Hemispheric asymmetry reduction in older adults: the HAROLD model. Psychol Aging 17:85–100.

Carp J, Park J, Polk TA, Park DC (2010) Age differences in neural distinctiveness revealed by multi-voxel pattern analysis. Neuroimage. Advance online publication. Retrieved April 21, 2010. doi:10.1016/jneuroimage.2010.04.267.

Chee MW, Goh JO, Venkatraman V, Tan JC, Gutchess A, Sutton B, Hebrank A, Leshikar E, Park D (2006) Age-related changes in object processing and contextual binding revealed using fMR adaptation. J Cogn Neurosci 18:495–507.

Christensen H, Mackinnon AJ, Korten AE, Jorm AF, Henderson AS, Jacomb P, Rodgers B (1999) An analysis of diversity in the cognitive performance of elderly community dwellers: individual differences in change scores as a function of age. Psychol Aging 14:365–379.

De Martino F, Valente G, Staeren N, Ashburner J, Goebel R, Formisano E (2008) Combining multivariate voxel selection and support vector machines for mapping and classification of fMRI spatial patterns. Neuroimage 43:44–58.

D'Esposito M, Deouell LY, Gazzaley A (2003) Alterations in the BOLD fMRI signal with ageing and disease: a challenge for neuroimaging. Nat Rev Neurosci 4:863–872.

Eger E, Ashburner J, Haynes JD, Dolan RJ, Rees G (2008) fMRI activity patterns in human LOC carry information about object exemplars within category. J Cogn Neurosci 20:356–370.

Folstein MF, Folstein SE, McHugh PR (1975) Mini-mental state—practical method for grading cognitive state of patients for clinician. J Psychiatric Res 12:189–198.

Gazzaley A, Cooney JW, Rissman J, D'Esposito M (2005) Top-down suppression deficit underlies working memory impairment in normal aging. Nat Neurosci 8:1298–1300.

Goh JO, Suzuki A, Park DC (2010) Reduced neural selectivity increases fMRI adaptation with age during face discrimination. Neuroimage 51:336–344.

Grady CL, Maisog JM, Horwitz B, Ungerleider LG, Mentis MJ, Salerno JA, Pietrini P, Wagner E, Haxby JV (1994) Age-related changes in cortical blood flow activation during visual processing of faces and location. J Neurosci 14:1450–1462.

Guyon I, Elisseeff A (2003) An introduction to variable and feature selection. J Machine Learn Res 3:1157–1182.
Hanson SJ, Halchenko YO (2008) Brain reading using full brain support vector machines for object recognition: there is no "face" identification area. Neural Comput 20:486–503.
Haxby JV, Gobbini MI, Furey ML, Ishai A, Schouten JL, Pietrini P (2001) Distributed and overlapping representations of faces and objects in ventral temporal cortex. Science 293:2425–2430.
Haynes JD, Rees G (2006) Decoding mental states from brain activity in humans. Nat Rev Neurosci 7:523–534.
Hultsch DF, MacDonald SW, Dixon RA (2002) Variability in reaction time performance of younger and older adults. J Gerontol B Psychol Sci Soc Sci 57:P101–P115.
Kamitani Y, Tong F (2005) Decoding the visual and subjective contents of the human brain. Nat Neurosci 8:679–685.
Li SC, Sikström S (2002) Integrative neurocomputational perspectives on cognitive aging, neuromodulation, and representation. Neurosci Biobehav Rev 26:795–808.
Li SC, Lindenberger U, Sikström S (2001) Aging cognition: from neuromodulation to representation. Trends Cogn Sci 5:479–486.
Li S, Ostwald D, Giese M, Kourtzi Z (2007) Flexible coding for categorical decisions in the human brain. J Neurosci 27:12321–12330.
Norman KA, Polyn SM, Detre GJ, Haxby JV (2006) Beyond mind-reading: multi-voxel pattern analysis of fMRI data. Trends Cogn Sci 10:424–430.
Park DC, Lautenschlager G, Hedden T, Davidson NS, Smith AD, Smith PK (2002) Models of visuospatial and verbal memory across the adult life span. Psychol Aging 17:299–320.
Park DC, Polk TA, Park R, Minear M, Savage A, Smith MR (2004) Aging reduces neural specialization in ventral visual cortex. Proc Natl Acad Sci U S A 101:13091–13095.
Park DC, Polk TA, Hebrank AC, Jenkins LJ (2010) Age differences in default mode activity on easy and difficult spatial judgment tasks. Front Hum Neurosci 3:75.
Payer D, Marshuetz C, Sutton B, Hebrank A, Welsh RC, Park DC (2006) Decreased neural specialization in old adults on a working memory task. Neuroreport 17:487–491.
Reitan R, Wolfson D (1993) The Halstead-Reitan neuropsychological test battery: theory and clinical interpretation, Ed 2. Tucson, AZ: Neuropsychology.
Reuter-Lorenz P (2002) New visions of the aging mind and brain. Trends Cogn Sci 6:394.
Salthouse TA (1996) The processing-speed theory of adult age differences in cognition. Psychol Rev 103:403–428.
Salthouse TA, Babcock RL (1991) Decomposing adult age differences in working memory. Dev Psychol 27:763–776.
Wechsler D (1981) Wechsler Adult Intelligence Scale-revised. Cleveland: The Psychological Corporation.
Zachary RA (1986) Shipley Institute of Living Scale, revised manual. Los Angeles: Western Psychological Services.
Zarahn E, Rakitin B, Abela D, Flynn J, Stern Y (2007) Age-related changes in brain activation during a delayed item recognition task. Neurobiol Aging 28:784–798.